Int J Adv Manuf Technol (2010) 46:945–956
DOI 10.1007/s00170-009-1940-z

SPECIAL ISSUE - ORIGINAL ARTICLE

A 32×32 temperature and tactile sensing array using PI-copper films

Y.-J. Yang · M.-Y. Cheng · S.-C. Shih · X.-H. Huang · C.-M. Tsao · F.-Y. Chang · K.-C. Fan

Received: 16 December 2007 / Accepted: 19 January 2009 / Published online: 7 February 2009

Abstract The development of a flexible 32×32 temperature and tactile sensing array, which will serve as the artificial skin for robot applications, is presented in this work. Pressure conductive rubber is employed as the tactile sensing material, and discrete temperature sensor chips are employed as the temperature sensing cells. Small disks of pressure conductive rubber are bonded on predefined interdigital copper electrode pairs which are patterned on a flexible copper–polyimide substrate which is fabricated by micromachining techniques. This approach can effectively reduce the crosstalk between each tactile sensing element. The mechanical and electrical properties of tactile sensing elements are measured. Also, the corresponding scanning circuits are designed and implemented. The temperature and tactile sensing elements are heterogeneously integrated on the flexible substrate. By using the integrated 32×32 sensing arrays, temperature and tactile images induced by the heaters/stamps of different shapes have been successfully measured. The flexible sensor arrays are bendable down to a 4-mm radius without any degradation in functionality.

Keywords Artificial skin · Flexible electronics · Micromachining · Tactile sensing array · Temperature sensing array

Y.-J. Yang (✉) · M.-Y. Cheng · S.-C. Shih · X.-H. Huang · C.-M. Tsao · K.-C. Fan
Department of Mechanical Engineering,
National Taiwan University,
Taipei, Taiwan
e-mail: yjy@ntu.edu.tw

F.-Y. Chang
Industrial Technology Research Institute,
Hsin-Chu, Taiwan

1 Introduction

The development of humanoid robots has been very popular recently. Intelligent sensing capabilities of humanoid robots are critical for effective and safe interactions between robots and humans. Therefore, the research on artificial skins used for robotic applications has received significant attention. The primary purposes of artificial skins are to realize the information exchange between robot and human beings as well as environment and to serve as the sensing systems to avoid damages to humans or robots. The basic sensing capabilities of an artificial skin include the sense of touch, the sense of temperature, and so on. For a typical artificial skin, a large number of sensing elements, such as tactile sensors and temperature sensors, are required to be implemented on a flexible-sheet structure of about few hundred centimeters square area. Also, an artificial skin should have enough flexibility to cover a three-dimensional surface.

Most previous works of sensor arrays employed silicon-based micro-electro-mechanical systems (MEMS) micromachining techniques on silicon substrate [1, 2]. However, silicon material in general is too brittle to sustain large deformation and thus is not suitable as the substrate material for flexible skins. In order to ensure sensor arrays to sustain sudden impact or large deformation, many research works using flexible substrate material have been proposed. The typical way to create a flexible substrate for sensing arrays is to spin-coat polyimide (PI) film on a carrier wafer, such as a silicon wafer or glass wafer. Then, micromachining techniques are employed to fabricate sensing elements on the PI film. Finally, flexible sensing array is realized by peeling off the PI film from the carrier wafer [3–6]. In [7], a flexible tactile sensing array is created by stitching thin metal wires on a conductive polymer-

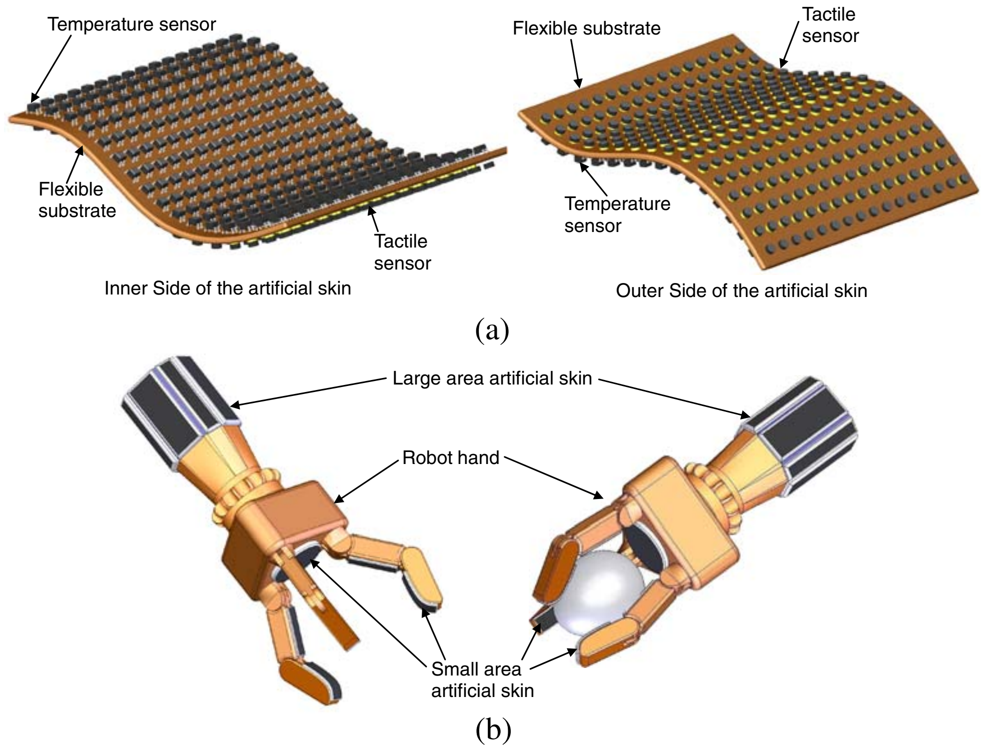

Fig. 1 **a** Schematic of the artificial skin proposed in this work. **b** Schematic of the applications of artificial skins

based flexible sheet. The stitched wires are carefully arranged to function as the sensing electrodes and the signal interconnects of the sensing array. Tajima et al. [8] employed MEMS manufacturing techniques to fabricate multilevel touch sensing systems on a flexible substrate, which can be used to cover wide areas of robot surfaces. Hasegawa et al. [9] developed a novel type of fabric tactile sensor which is made from hollow flexible fibers consisting of electrically conductive fabric and string. In [10], tactile sensing array were formed by wiring bonding discrete pressure sensor dies on a flexible printed circuit board. In [11, 12], tactile sensing arrays were implemented using capacitive sensing mechanism. Also, Someya et al. [13] fabricated flexible tactile and temperature sensing arrays using organic materials. Furthermore, in [12–15], temperature sensing arrays were also integrated with the tactile sensing arrays.

In this paper, we present the development of an artificial skin which is realized by heterogeneously integrating tactile sensing elements and the temperature sensing elements on a flexible substrate. The major advantages of our approach are low-cost and easy for fabricating large-area sensing array. The flexible substrate is fabricated using micromachining techniques. Pressure-conductive rubber is used

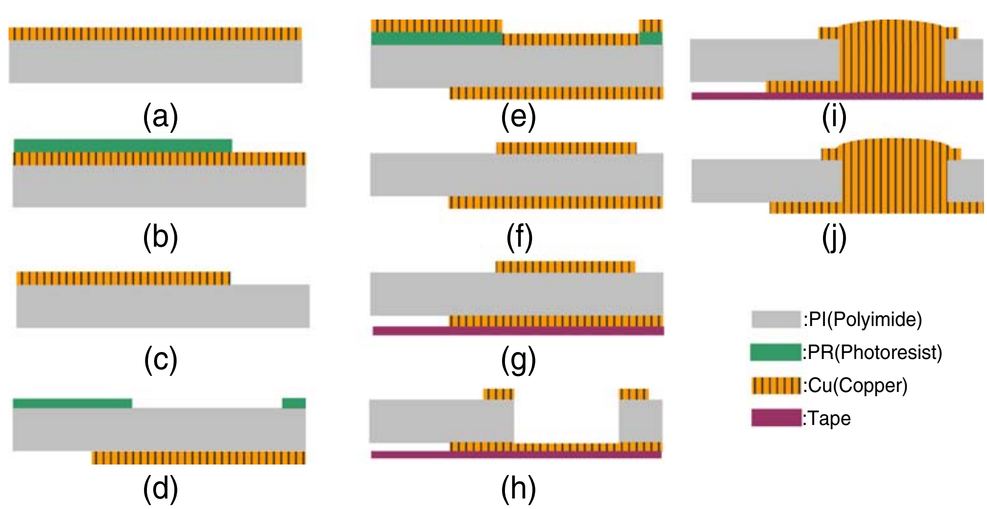

Fig. 2 The micromachining process flow of the skin structure of sensing arrays

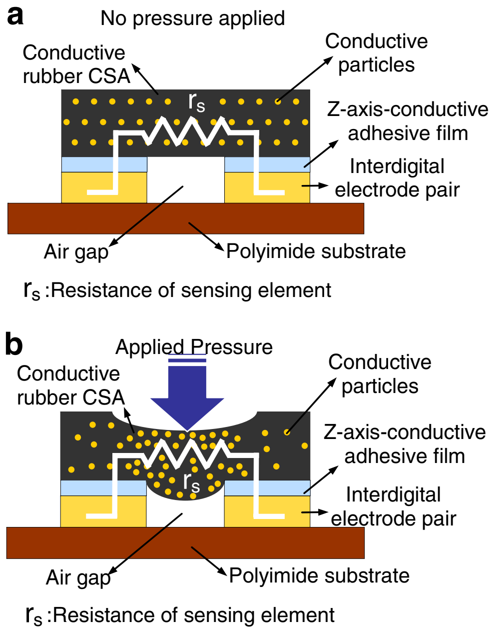

Fig. 3 **a** Schematic of a tactile sensing element without applied pressure. **b** Schematic of a tactile sensing element under compression

as the sensing elements for tactile sensor arrays. A simple method for fabricating reliable tactile sensing elements is also proposed. This approach gives excellent electrical isolation between each tactile sensing element. Furthermore, discrete temperature sensor chips are used to form temperature array which gives accurate temperature distribution of the skin.

This paper is organized as follows: the design and fabrication of sensor arrays are described in Section 2. Section 3 presents the scanning circuits for temperature and tactile sensing arrays. In addition, a split-scanning module is also described in this section. Measured results will be presented in Section 4. Finally, Section 5 draws conclusions.

2 Design and fabrication of sensor arrays

2.1 Skin structure

In this research, we will focus on the development of a low-cost artificial skin which is realized by integrating tactile temperature on a flexible substrate. Figure 1a shows the schematic of the proposed artificial skin. One side of the flexible substrate will be exposed to the environment for signal acquisition. On this side (i.e., the outer side of the skin), a patterned copper layer serves as the interdigital electrodes for pressure-conductive rubber, which will be used as the tactile sensing material. On the other side of the substrate (i.e., the inner side of the skin), a patterned copper layer serves as the contact pad for bonding discrete temperature sensing chips. Figure 1b illustrates the applications of the skin. The tactile sensing array can be used to measure the force distribution as the robot hand squeezes an object. The temperature sensing capability can be used to avoid danger of heat. Also, the temperature sensing array can be deployed on the fingers of a robot hand for measuring the temperature distribution of the object holding by the fingers.

Figure 2 shows the micromachining process flow for fabricating flexible skin substrate. The starting material is a flexible substrate which is in fact a polyimide film with copper layer on one side [16]. The thicknesses of the PI layer and the copper layer are 35 and 25 µm, respectively. The copper layer, which is on the inner side of the skin, is patterned to form the column interconnects and the soldering pads for the temperature sensor chips (step b and step c). On the outer side of the skin, the row interconnect and the electrodes for tactile sensing elements are created by lifting off a copper film (2 µm) which is deposited by e-beam evaporation (step d, step e, and step f). Then, scotch tape is attached on the inner

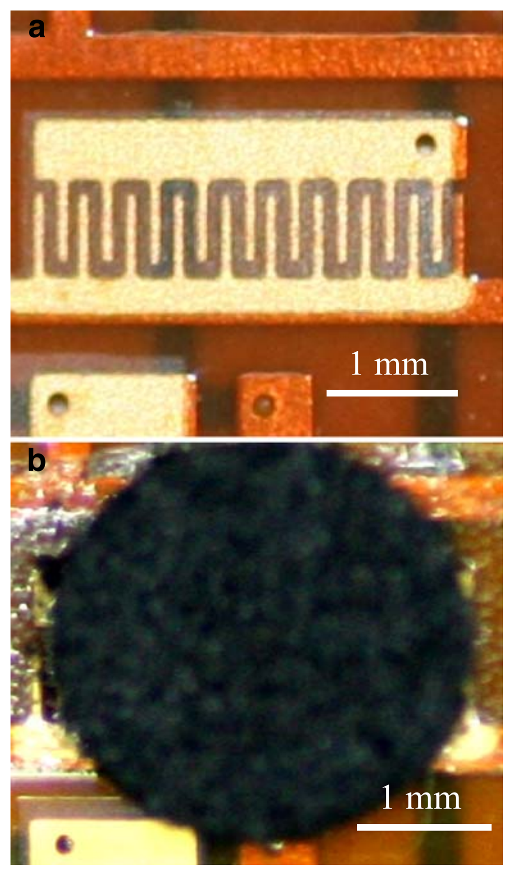

Fig. 4 **a** Fabricated interdigital electrodes for the tactile sensing elements. **b** Electrodes bonded with a punched CSA disk using *Z*-axis-conductive adhesive film

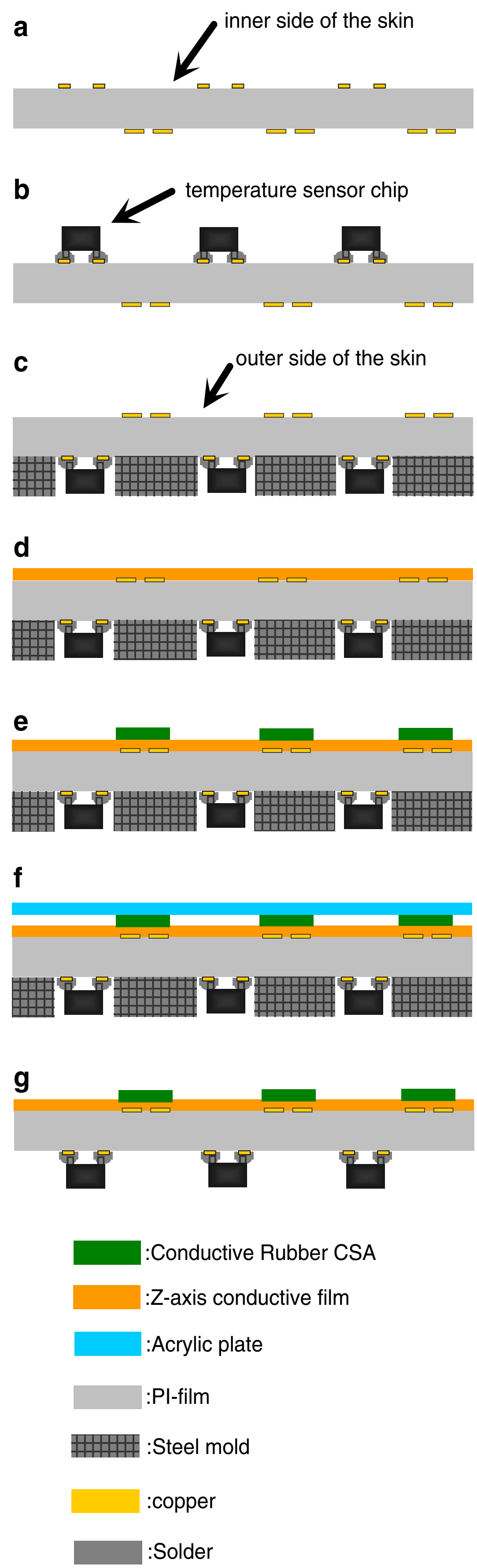

Fig. 5 Process flow of temperature and tactile sensing arrays heterogeneously integrated on a flexible copper-PI film

side of the skin in order to protect the device for drilling process (step g and step h). The drilled holes (via-holes) are filled with copper using electroplating process (step i). Finally, the tape is removed and the flexible skin structure is ready for implementing temperature and tactile sensing elements.

2.2 Tactile sensing elements

Various properties, such as flexibility, durability, and low hysteresis, are essential for the tactile sensing material used for artificial skins. The most common materials are silicon-conductive rubber [17], thermoplastic semi-conductive ink [18], and pressure-conductive rubber [19]. The major drawbacks of silicon-conductive rubber are high hysteresis, high noise, and low sensitivity. On the other hand, sensing elements made by thermoplastic semi-conductive ink are usually not durable. In this work, we employ CSA (pressure-conductive rubber CSA, PCR Technical) [20] as the sensing material for the tactile sensing array. This material, which is made by mixing elastomer with carbon particles, is a flexible gray black sheet with 0.5-mm thickness. The CSA behaves like an insulator when no pressure is applied, while its electrical resistance reduced significantly under compression. Figure 3a shows the working principle of CSA. As no pressure is applied, the conductive particles are uniformly distributed in CSA without contacting each other, which makes CSA like an insulator. As CSA is compressed, as shown in Fig. 3b, the conductive particles contact each other so that its resistivity decreases. The resistance decreases as the applied pressure increases.

In order to measure the CSA resistance under applied pressure, a small circular piece of CSA is placed on an electrode pair which is patterned on the flexible substrate described in previous subsection. Note that a *Z*-axis-conductive adhesive film (3M™ electrically conductive adhesive transfer tape 9703) [21] is used to bond the CSA with the electrode pair. Figure 4a shows a fabricated interdigital electrode pairs for tactile sensing elements, and Fig. 4b is the picture of the pair bonded with a small piece of CSA disk using the *Z*-axis-conductive adhesive film.

It has to be emphasized that when conductive rubber materials (e.g., CSA) are used for tactile sensing array, the most typical approach is to bond a large-area conductive polymer sheet [22–24] on a substrate patterned with an array of electrode pairs. This approach is relatively straightforward for fabrication. However, the tactile sensing array made by this approach usually has very large cross-talks between adjacent sensing elements. A few methods have been proposed to minimize cross-talk currents [7, 25, 26]. In this work, we reduce cross-talk current by using small isolated CSA disks which are punched from a CSA sheet. The size of punched CSA disks is about the size of each interdigital electrode pair. Since CSA disks are isolated from each other, electrical current leakages through adjacent CSA disks can be effectively reduced.

2.3 Integration of tactile and temperature sensing arrays

Figure 5 shows the process flow of heterogeneously integrating the tactile and temperature sensing arrays on the flexible copper–PI film. The starting material is the flexible skin structure described in previous subsection. The inner side of the skin structure faces up, as shown in Fig. 5a. Firstly, temperature sensor chips, MAX6607 (in SC70 package) [27], are soldered on the corresponding contact pads on the inner side of the skin (Fig. 5b). The temperature sensor chips is quite accurate (±0.7°C from 0°C to +70°C) and the required voltage is relatively small (1.8 to 3.6 V). Then, the skin is flipped so that its outer side faces up, as shown in Fig. 5c. Also, the skin is placed above a steel plate which has 32×32 drilled holes. The steel plate will serve as the handling platform for avoiding damaging the soldered chips during the process of implementing tactile sensing elements on the outer side of the skin. Then, the *Z*-axis-conductive adhesive film is placed above the skin (Fig. 5d) and punched CSA disks are attached above each interdigital electrode pair (Fig. 5e). In order to ensure that all the CSA disks are electrically bonded with interdigital electrode pairs, the whole sensor array is pressed at 0.1 MPa using a thin acrylic flat plate for 24 h (Fig. 5f). This process is also essential to avoid non-uniform pressure sensitivity between each sensing element, resulting in inaccurate pressure distribution during operation. Finally, the steel handling plate is removed and the fabricated device is shown in Fig. 5g.

Figure 6a shows that CSA disks are punched from a CSA sheet using a seamless steel tube with 3-mm inner diameter. Figure 6b shows that the punched CSA disks are attached on the interdigital electrode pair using the *Z*-axis-conductive adhesive film. Then, all CSA disks are pressed at 0.1 MPa using a thin acrylic plate, as shown in Fig. 6c. Figure 6d is the picture of the fabricated tactile array. Figure 7a shows the fabricated artificial skin with temperature and tactile sensing elements. The flexibility of the device is also demonstrated. The outer and inner sides of the skin are shown in Fig. 7b, c, respectively. As shown in the figure, on the outer side of the skin, punched CSA disks on the predefined interdigital electrode pairs are employed as the tactile sensing elements. Discrete temperature sensor chips are soldered on the inner side of the skin. Since the temperature sensor chip detects

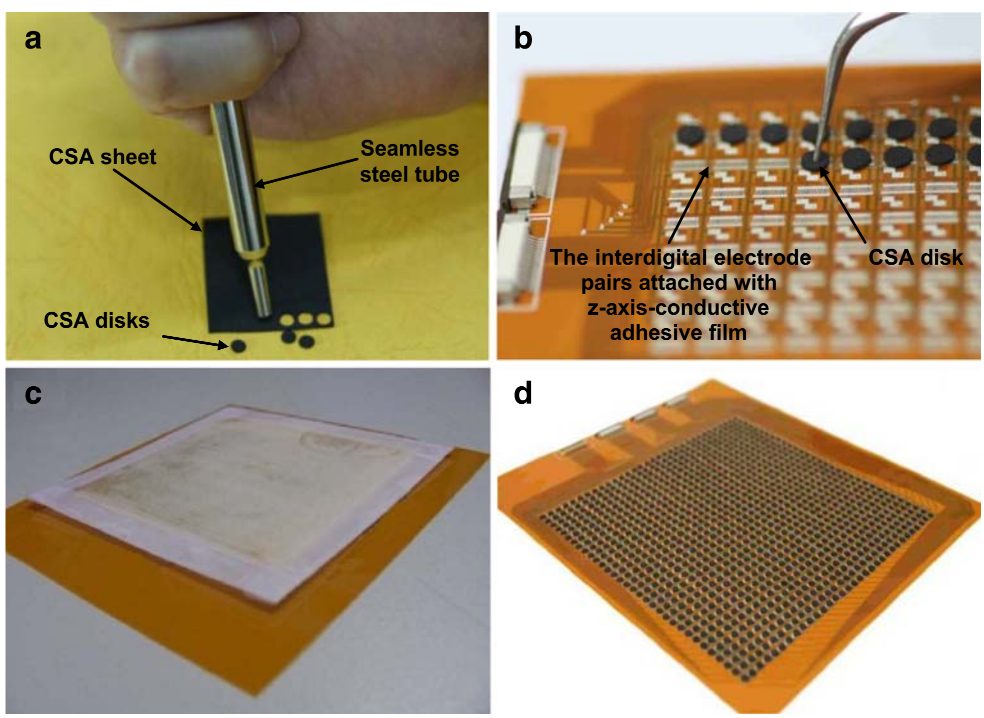

Fig. 6 **a** CSA disks can be punched by using a seamless steel tube. **b** The CSA disk is attached to the interdigital electrode pairs. **c** The acrylic plate is used to press all sensors on the interdigital electrode pairs. **d** Fabricated tactile sensing array

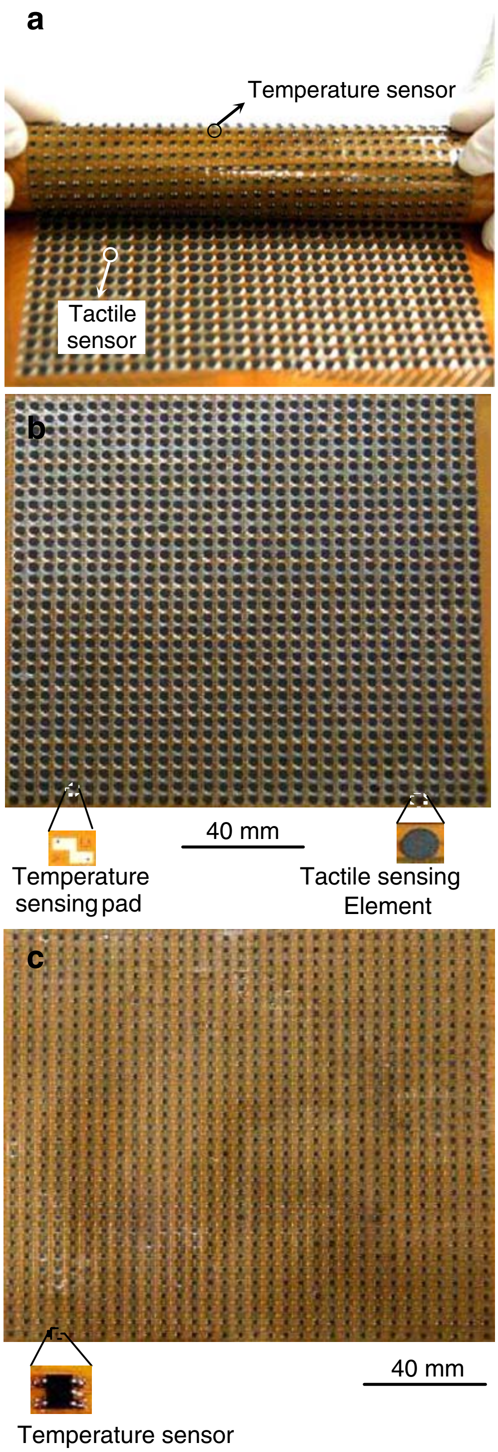

Fig. 7 **a** Fabricated artificial skin with two sensing arrays. **b** Outer side of the skin (the tactile sensing array). **c** Inner side of the skin (the array of temperature sensor chips)

temperature most effectively by its metal leads, the environment temperature on the outer side of the skin can be accurately measured through the via-holes which are filled with electroplated copper.

3 Scanning systems

3.1 Scanning circuits

Figure 8 is the schematic of a 32×32 sensing array system, which includes the temperature and tactile sensing arrays as well as the corresponding scanning circuits. For row scanning, a set of multiplexers provides the driving power to sensing elements. For column scanning, another set of multiplexers is used to receive the data outputs from each sensor. For the temperature sensing array, the scanning circuit directly measures the voltage output of each temperature sensor chip. For the tactile sensing array, the scanning circuit measures the resistance change of each sensing element. A constant voltage is supplied, and the change of the current flowing through the resistor can be detected by the current-to-voltage converter, as shown in the figure. The scanned output voltages of the temperature and tactile sensing arrays are transferred to their corresponding MCU by an analog-to-digital converter. Scanning requests for each sensing array can be made by a PC through serial communication port (RS-232). Also, the scanned data can be transferred to the PC through RS-232 for visualization and data analysis. The maximum scanning rate is greater than 3,000 elements per second. Figure 9a shows the picture of the whole 32×32 scanning circuits system, which includes an RS-232 switch circuit, a 32×32 temperature scanning circuit, and a 32×32 tactile scanning circuit. Figure 9b is the picture of the fabricated artificial skin and the scanning circuit system.

3.2 Split-scanning module

The requirement of the sensing array sizes is usually based on applications. For example, for a robot hand, many 8×8 sensing arrays are required to cover each finger, while a 32×32 sensing array is needed to cover a robot arm. In other words, it is desirable that the resolution and size of sensing arrays can be easily tailored to the applications' requirements. Therefore, it will be extremely advantageous if one 32×32 scanning circuit can also be used for scanning many smaller sensing arrays simultaneously. In this work, we develop a split-scanning module which splits the 32×32 scanning row/column signal leads (R_{01}–R_{32} and C_{01}–C_{32}) into four sets of 16×16 scanning row/column signal leads. The schematic of the system with the split-scanning module is shown in Fig. 10. On the split-scanning module, port X is connected to the 32×32 scanning circuit. Port Y is the duplicate port of port X, while the signal leads of port A, port B, port C, and port D are in fact the four smaller sets split from the signal leads of port X. The splitting of signal leads can be easily

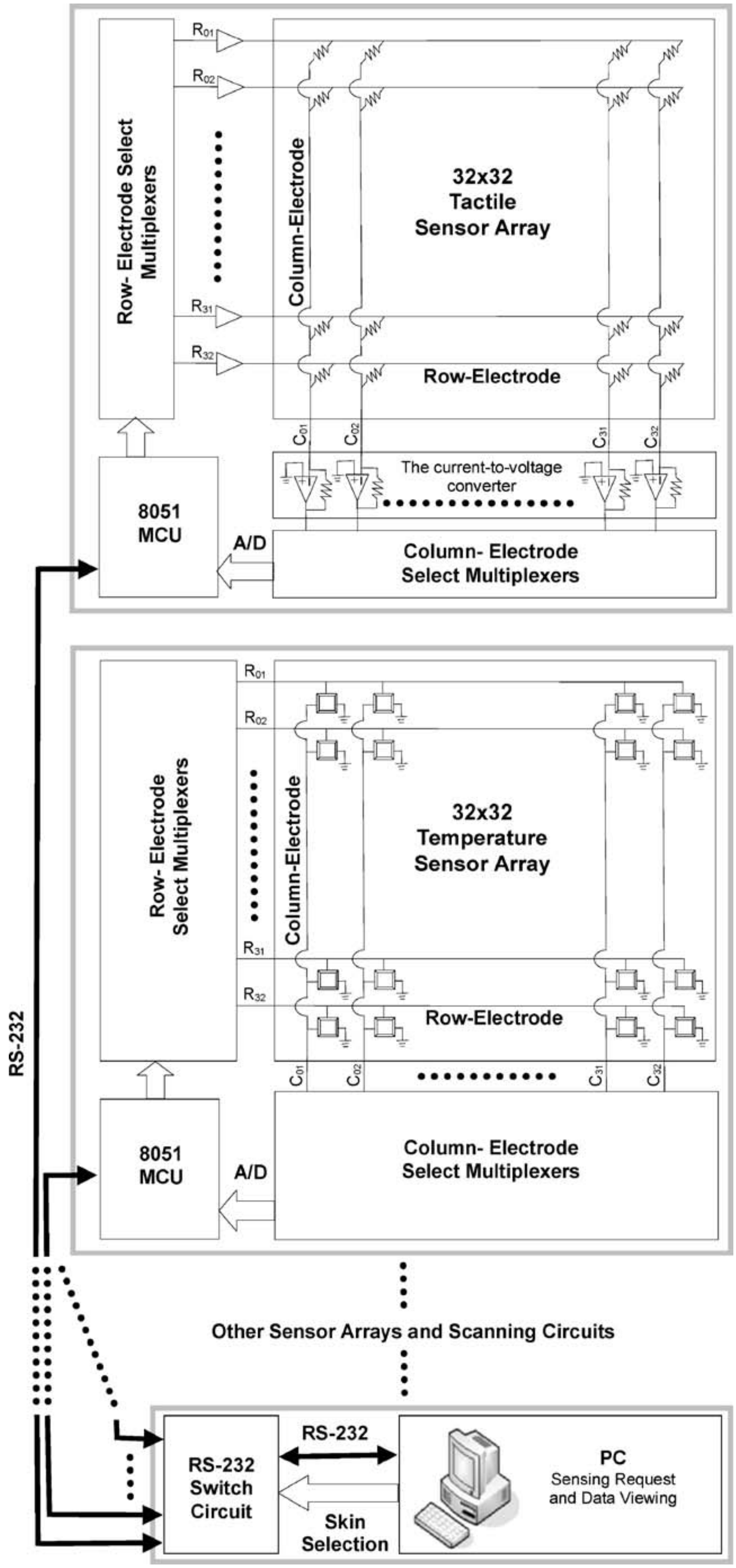

Fig. 8 Schematic of the sensing array system

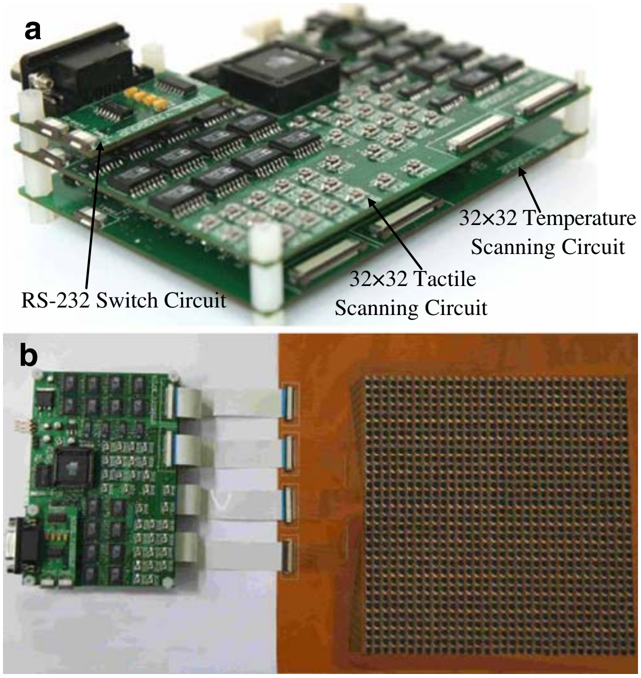

Fig. 9 **a** Schematic of scanning circuit system. **b** Fabricated artificial skin and scanning circuit system

achieved by a double-side printed circuit board. In Fig. 10a, a 32×32 sensor array can be connected to port Y. In Fig. 10b, four 16×16 sensor arrays are connected to ports A–D and can be scanned by the 32×32 scanning circuit simultaneously. Note that the combinations of row/column signal leads for ports A–D are also indicated in Fig. 10. By using the split-scanning module, many smaller arrays of sensors can be scanned by a single 32×32 scanning circuit. Figure 11 shows a few fabricated skins with different array sizes.

4 Measurement and discussion

The measurement setup for characterizing tactile sensing element can be found in [14]. The measured relationships of resistance vs. applied pressure for the CSA materials are shown in Fig. 12a. The curve in the figure is the average result by measuring one sample sheet 50 times with different applied pressure. The error bars indicate the measured maximum and minimum values. The relationship between the applied load and the deformation of the CSA is shown in Fig. 12b. Note that the measured CSA is punched into a circular shape with 3-mm diameter and 0.5-mm thickness. Based on the measured results, the Young's module of the CSA is estimated as 1,450 kPa. The fabricated flexible sensor arrays are bendable down to a 4-mm radius without any degradation in functionality.

Aluminum heaters of different shapes and the measured temperature distributions caused by these heaters are shown in Fig. 13. These heaters, which are 10 mm in thickness, are put on a hot plate with 70°C for 1 min

Fig. 10 Configurations of sensing array systems using a split-scanning module and a 32×32 scanning circuit. **a** The system with one 32×32 sensing array. **b** The system with four 16×16 sensing arrays

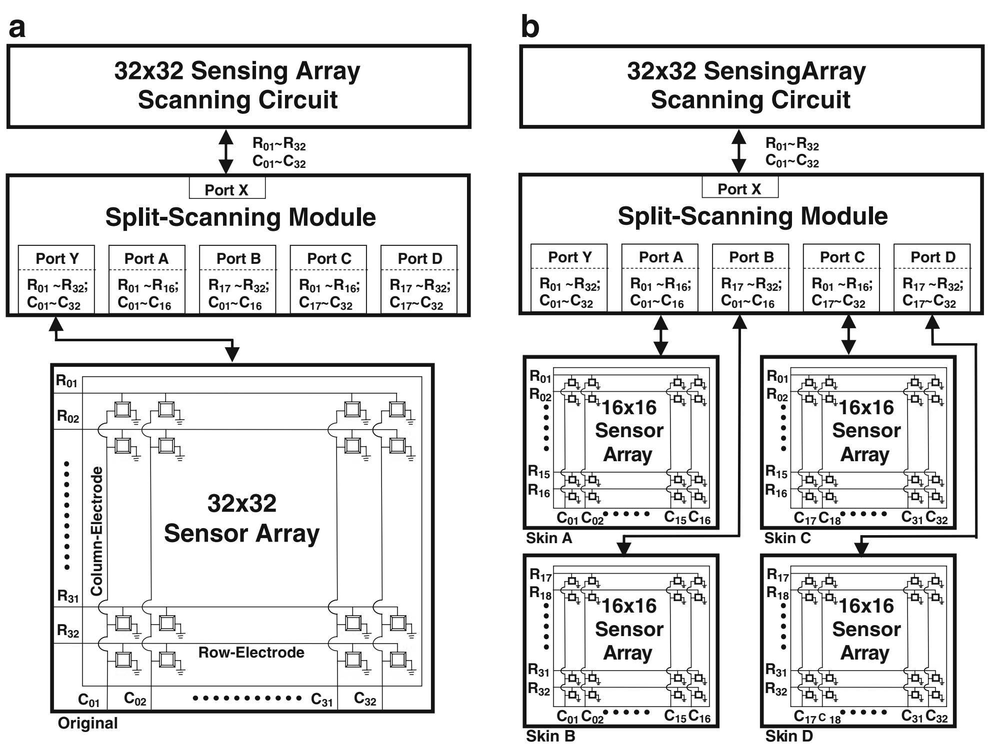

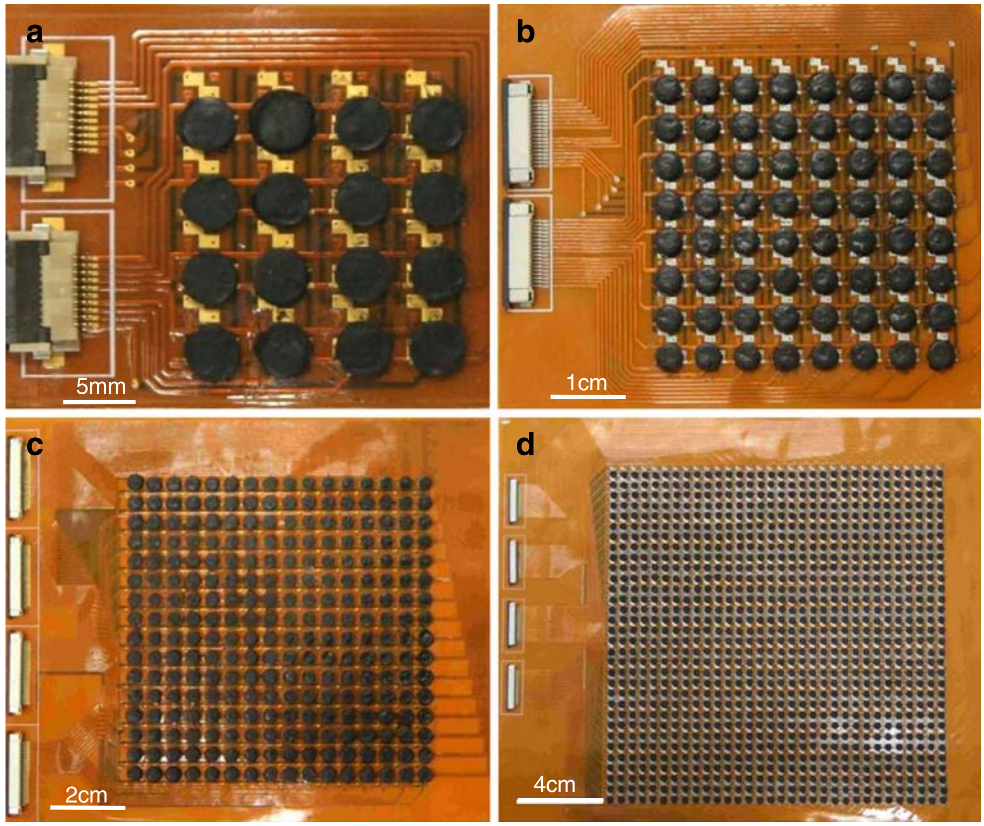

Fig. 11 Various array sizes of artificial skins. **a** 4×4 sensing array. **b** 8×8 sensing array. **c** 16×16 sensing array. **d** 32×32 sensing array

before they are placed above the sensing array. During the measurement, the distance between the heaters and the sensor array is about 1 mm. Note that the sensitivity of the temperature sensor chip is 0.01 V/°C [27]. Obviously, the heaters of different shapes, including the triangular shape, the star shape, the square shape, and the alphabet letters "NTU", are clearly resolved by the temperature sensor array. The measured pressure distributions using acrylic stamps of different patterns are shown in Fig. 14. The figure also shows the pictures and dimensions of these stamps. For Fig. 14a, b, the applied pressure is produced by placing a 3-kg weight on top of the stamps. Similarly, a 2-kg weight is used for Fig. 14c, d. Note that two-dimensional sensing images of the temperature and pressure measurement are obtained using 32×32 sensing arrays. Hand pattern is one of the human characteristics which can be used to recognize human identity. By using the developed sensor array, the patterns of human palm and fingers can be extracted from the pressure and temperature images, as shown in Fig. 15.

5 Conclusion

In this work, the design, fabrication, and measurement of a flexible sensor array system is presented. The sensor array, which is composed of a 32×32 temperature sensing array

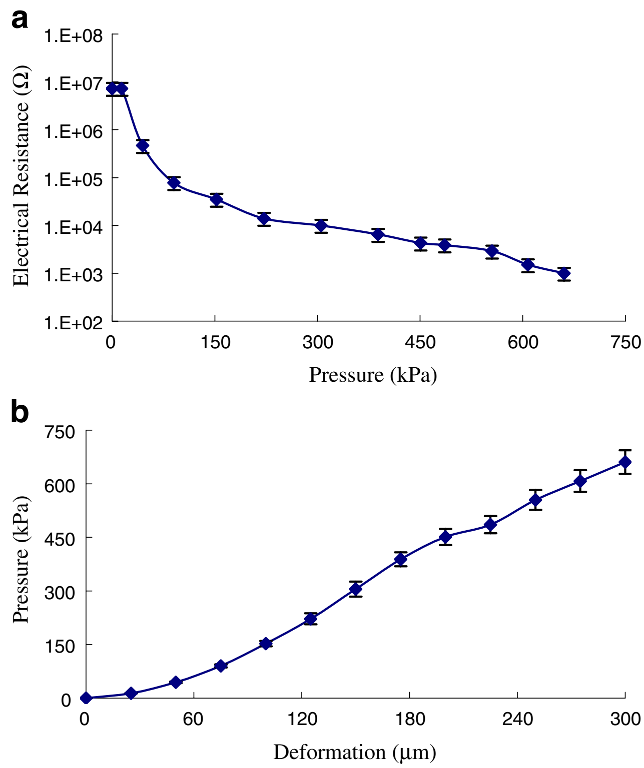

Fig. 12 **a** Measured relationship of resistance vs. applied pressure for the CSA. **b** Measured relationship of the deformation of the CSA vs. applied pressure. Note that the measured CSA is punched as a circular shape with 3-mm diameter and 0.5-mm thickness

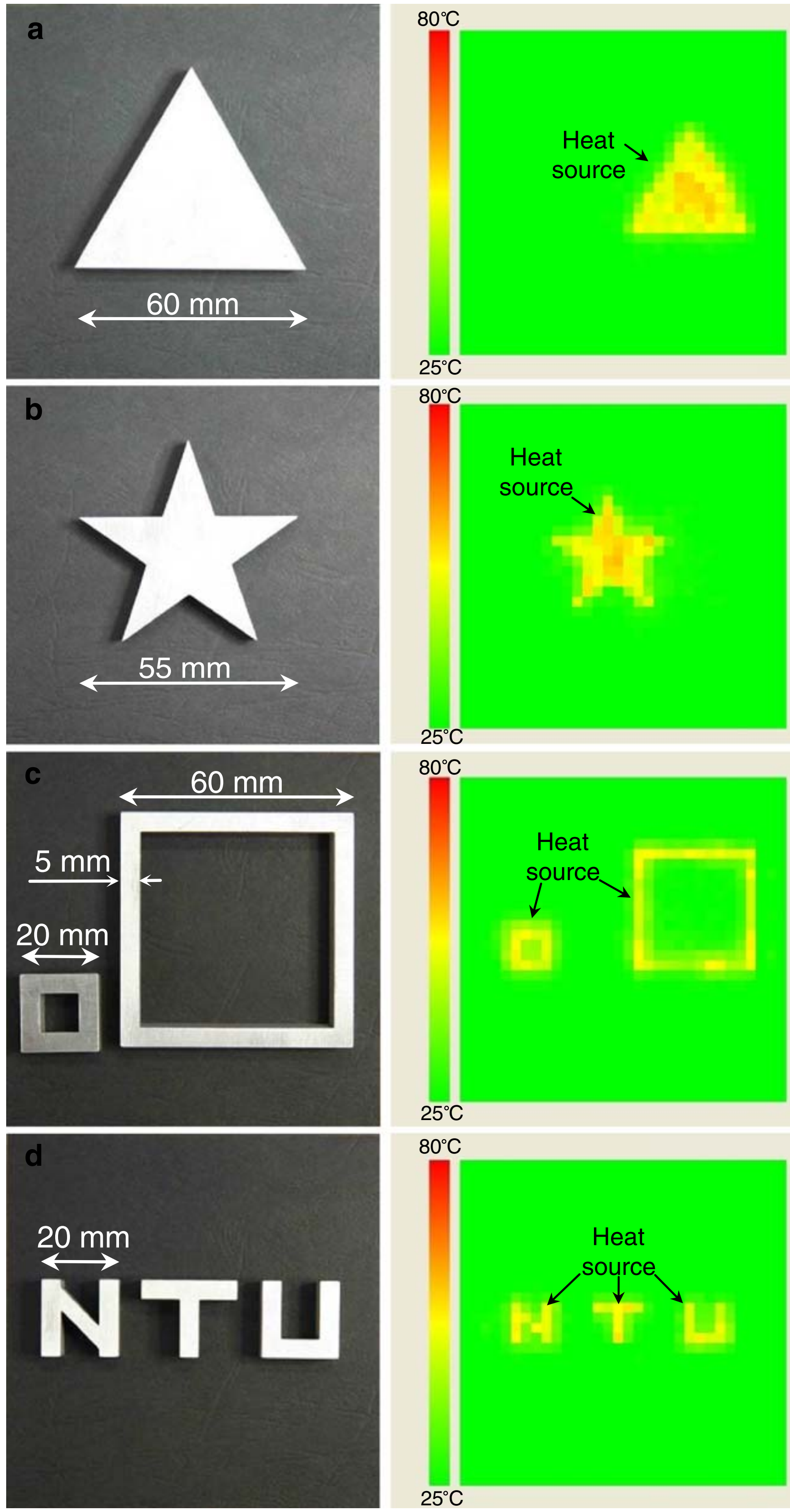

Fig. 13 Heaters of different shapes and the measured temperature distributions caused by these heaters. The distance between the sensor array and the heaters is about 1 mm

and an 32×32 tactile sensing array, will be used as the artificial skin for robot applications. The tactile and temperature sensing elements are heterogeneously integrated on a flexible substrate which is fabricated using micromachining techniques. In order to reduce the cross-talk between each tactile sensing element, small disks of CSA are bonded on interdigital electrode pairs individually. Discrete temperature sensor chips, which

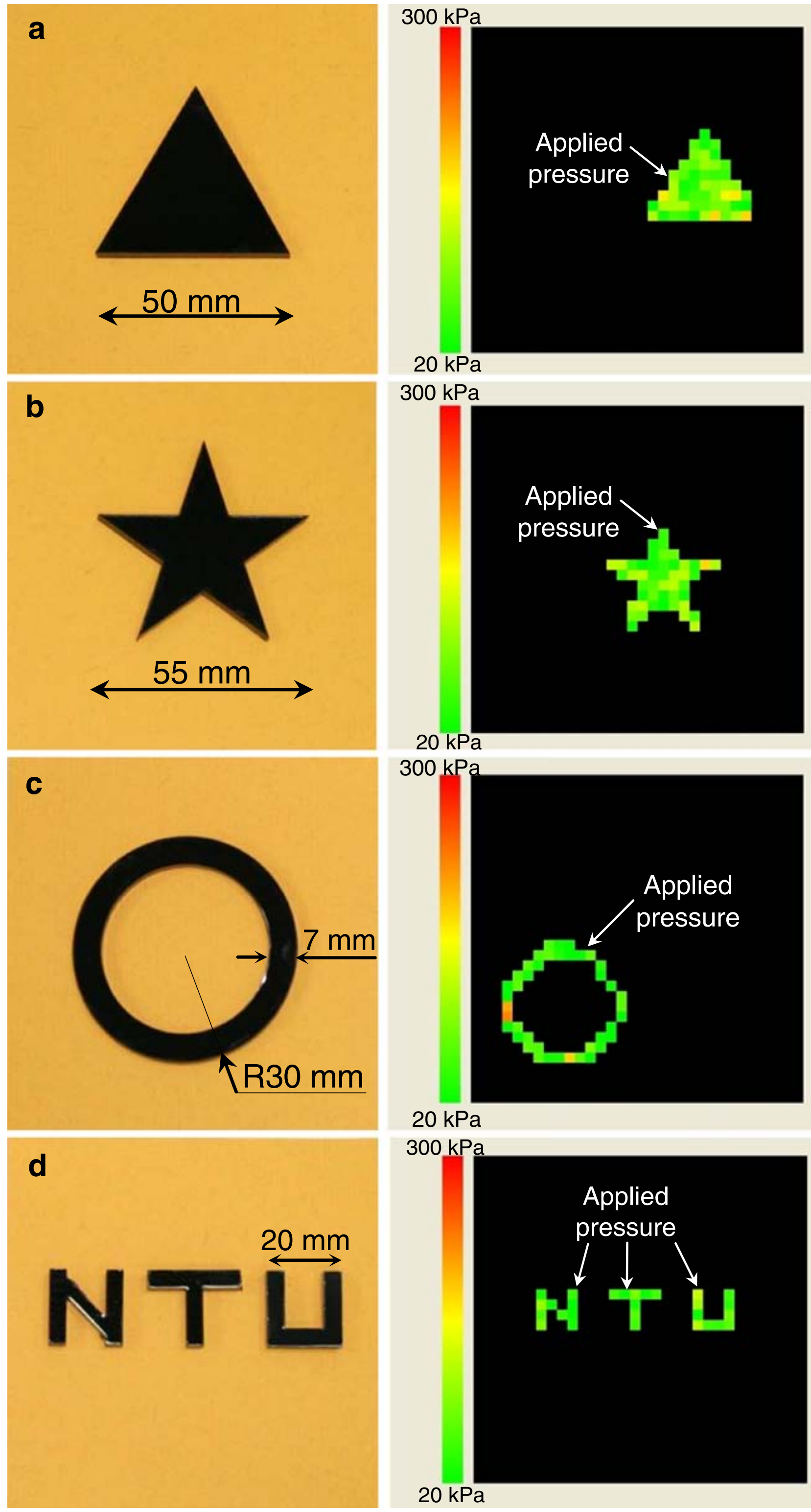

Fig. 14 Measured pressure distributions using solid stamps of different patterns. The acrylic stamps are also shown

serve as the temperature sensing elements, are soldered on the flexible substrate. The corresponding 32×32 scanning circuit for each sensing array is designed and implemented. A split-scanning module, which gives the function flexibility of the 32×32 scanning circuits, is proposed and designed. Measured results of temperature and pressure distributions using heaters/stamps of different shapes are also presented.

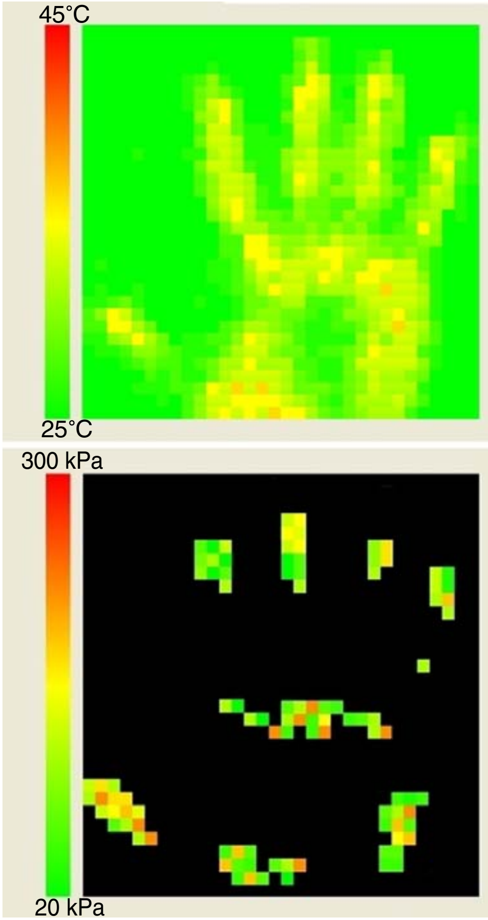

Fig. 15 Measured temperature and pressure distributions of a human right hand

Acknowledgment This project is sponsored by the ITRI, Taiwan, Republic of China. The authors would like to thank for Bonnie T.-T. Chia for help on flexible substrate fabrication.

References

1. Kane BJ, Cutkosky MR, Kovacs GTA (2000) A traction stress sensor array for use in high-resolution robotic tactile imaging. Journal of Microelectromechanical Systems 9(4):425–433
2. Wang L, Beebe DJ (2000) A silicon-based shear force sensor: development and characterization. Sens Actuators A 84:33–44
3. Engel J, Chen J, Liu C (2003) Development of polyimide flexible tactile sensor skin. J Micromech Microeng 13(3):359–366
4. Jiang F, Tai YC, Walsh K, Tsao T, Lee GB, Ho CM (1997) A flexible MEMS technology and its first application to shear stress sensor skin. Proceedings of IEEE MEMS'97, pp 465–470
5. Hwang ES, Seo JH, Kim YJ (2006) A polymer-based flexible tactile sensor for normal and shear load detection. Proceedings of IEEE MEMS'06, pp 714–717
6. Engel J, Chen J, Fan Z, Liu C (2005) "Polymer micromachined multimodal tactile sensors". Sens Actuators A 117(1):50–61
7. Shimojo M, Namiki A, Ishikawa M, Makino R, Mabuchi K (2004) A tactile sensor sheet using pressure conductive rubber with electrical-wires stitched method. IEEE J Sens 4(5):589–596
8. Tajima R, Kagami S, Inaba M, Inoue H (2002) Development of soft and distributed tactile sensors and the application to a humanoid robot. Adv Robot 16(4):381–397
9. Hasegawa Y, Shikida M,Ogura D, Sato K (2007) Novel type of fabric tactile sensor made from artificial hollow fiber. Proceedings of IEEE MEMS'07, pp 603–606
10. Kim K, Lee KR, Kim YK, Lee DS, Cho NK, Kim WH, Park KB, Park HD, Park YK, Kim JH, Pak JJ (2006) 3-Axes flexible tactile sensor fabricated by si micromachining and packaging technology. Proceedings of IEEE MEMS'06, pp 678–681
11. Lee HK, Chang SI, Yoon E (2006) A flexible polymer tactile sensor: fabrication and modular expandability for large area deployment. Journal of Microelectromechanical Systems 15 (6):1681–1686
12. Castelli F (2002) An integrated tactile-thermal robot sensor with capacitive tactile array. IEEE Trans 38(1):85–90
13. Someya T, Kato Y, Sekitani T, Iba S, Noguchi Y, Murase Y, Kawaguchi H, Sakurai T (2005) Conformable, flexible, large-area networks of pressure and thermal sensors with organic transistor active matrixes. Proc Natl Acad Sci USA 102(35):12321–12325
14. Cheng MY, Chang WY, Tsao LC, Yang SA, Yang YJ, Shih WP, Chang FY, Chang SH, Fan KC (2007) Design and fabrication of an artificial skin using PI-copper films. Proceedings of IEEE MEMS'07, pp 389–392
15. Shamanna V, Das S, Celik-Butler Z, Butler DP, Lawrence KL (2006) Micromachined integrated pressure-thermal sensors on flexible substrates. J Micromech Microeng 16:1984–1992
16. Datasheet of XSIE101020, Taiflex Scientific Inc. http://www.taiflex.com.tw/english/porducts_2.asp
17. Pugh A (1986) Robot sensors. FS Ltd, New York, pp 87–97
18. Papakostas TV, Lima J, Lowe M (2002) A large area force sensor for smart skin applications. Proc IEEE Sensors 2:1620–1624
19. Shida K, Yuji JI (1996) Discrimination of material property by pressure-conductive rubber sheet with multi-sensing function. Proceedings of IEEE International Symposium on Industrial Electronics. Warsaw, Poland, pp 54–59
20. Datasheet of pressure-conductive rubber CSA, PCR Technical Inc., http://pcr.lar.jp/e_hint_for_design.pdf
21. Datasheet of electrically conductive adhesive film, 3M Electronics Inc., http://www.mpsupplies.com/3MElectricallyCondutiveTape9703.pdf
22. Chalupa V, Marik V, Volf J (1983) Tactile matrix for shape recognition. Proceedings of the 9th IMEKO Congress of the International Measurement Confederation, vol 1, pp 339–348
23. Kerpa O, Weiss K, Worn H (2003) Development of a flexible tactile sensor system for a humanoid robot. IEEE International Conference on Intelligent Robots and Systems, pp 1–6
24. Freitag R, Meixner H (1988) PVDF sensor array for human body detection. Proceedings of IEEE 6th International Symposium. Oxford, England, pp 374–378
25. Ishikawa M, Shimojo M (1988) An imaging tactile sensor with video output and tactile image processing. The Society of Instrument and Control Engineers, pp 662–669
26. Takahashi Y, Nishiwaki K, Kagami S, Mizoguchi H, Inoue H (2005) High-speed pressure sensor grid for humanoid robot foot. Proceeding of IEEE International Conference on Intelligent Robots and Systems, pp 3909–3914
27. Datasheet of MAX-6607, Maxim Integrated Products Inc., http://datasheets.maxim-ic.com/en/ds/MAX6607-MAX6608.pdf